Mean field renormalization group for the spin-1/2 XXZ model

1992 J. Phys. A: Math. Gen. 25 4285

(http://iopscience.iop.org/0305-4470/25/16/007)

J. Phys. A: Math. Gen. 25 (1992) 4285–4296. Printed in the UK

Mean field renormalization group for the spin-$\frac{1}{2}$ XXZ model

Dirk Jan Bukman and J M J van Leeuwen

Instituut-Lorentz, Rijksuniversiteit te Leiden, PO Box 9506, 2300 RA Leiden, The Netherlands

Received 24 October 1991

Abstract. The mean field renormalization group (MFRG) method is applied to the spin-$\frac{1}{2}$ XXZ model. The phase diagram is obtained for various lattice structures in two and three dimensions, as well as estimates for the critical exponents. The results of the original MFRG method are quite good, but the more sophisticated approach that also includes surface exponents is not suitable for application to the small clusters used here.

1. Introduction

The mean field renormalization group (MFRG) method introduced by Indekeu *et al* [1, 2] has turned out to be a rather successful method for computing phase diagrams and critical properties of statistical models. The strength of this method lies in the fact that it gives quite good results (at least for the critical temperatures) at a relatively low computational cost. As a result it has been applied to a variety of classical and quantum spin systems. The relative simplicity of the method makes it possible to examine reasonably complicated models for a variety of lattice structures in two and three dimensions. In this paper we apply the MFRG method to the spin-$\frac{1}{2}$ XXZ model, and draw some conclusions about its value in this case.

The XXZ model is described by the reduced Hamiltonian

$$-\beta\mathcal{H} = \sum_{\langle ij \rangle} K(\sigma_i^x \sigma_j^x + \sigma_i^y \sigma_j^y) + K_z \sigma_i^z \sigma_j^z. \tag{1.1}$$

The sum $\sum_{\langle ij \rangle}$ is over nearest neighbour spins, and the σ_i^α are Pauli matrices. If the z-coupling K_z is positive (ferromagnetic), and larger than the xy-coupling K, the system has an Ising-like ferromagnetically ordered phase (FI), with a non-zero magnetization along the z-axis. If the xy-coupling dominates, there is an ordered phase with a magnetization in the xy-plane (XY). If K_z is negative (antiferromagnetic) an Ising-like phase with a non-zero staggered magnetization forms for bipartite lattices (AI). (For such lattices there is a symmetry between K and $-K$, and hence between the ferromagnetic and antiferromagnetic XY phases. We will always take K positive in this case.) A lattice that is not bipartite cannot accommodate such a phase due to the frustration of the lattice. We will not consider the phases that form under such circumstances. The FI phase has already been discussed by Plascak [3], and we will extend the calculation to include the other phases as well. It turns out that the

0305-4470/92/164285+12$04.50

behaviour of the MFRG *for the XY and* AI *phases is fundamentally different from that for the* FI *phase.*

Additional interest in the Hamiltonian (1.1) derives from the fact that it is equivalent to that of a lattice gas of interacting hard-core bosons [4, 5], and it has been used to describe both superfluidity and superconductivity.

2. The mean field renormalization group

In this section we will first describe the MFRG method as it applies to a simple Ising model, and then discuss the differences that arise when it is applied to the *XXZ* Hamiltonian (1.1). We calculate, for an Ising model with a coupling constant K and a magnetic field H, the magnetization m of a finite cluster containing N spins, e.g. one of the clusters shown in figure 1. The magnetization is calculated in the presence of a symmetry breaking boundary condition, so that the cluster is embedded in an effective magnetization m_0, simulating the influence of the surrounding infinite lattice. Because of this effective magnetization the spins on the boundary of the cluster experience an extra effective surface field $H_{\text{eff}} = \alpha K m_0$, with α the number of lattice points outside the cluster that are adjacent to a boundary spin. (We only consider clusters, as in figure 1, where all spins are boundary spins, and all spins are equivalent. A generalization for a case where this is not so is easily made.) The basic idea of the MFRG is to repeat this calculation for a different cluster of N' spins ($N' < N$), with different parameters K', H', and m_0', and view the results as if they were related by a scaling transformation.

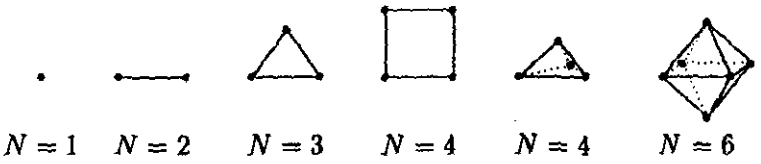

Figure 1. The clusters that are used in the calculation. The single site and the pair are used for all lattices; the triangle for the triangular and FCC lattices; the square for the square and cubic lattices; the tetrahedron and the octahedron for the FCC lattice.

Postulating finite size scaling for the two clusters leads to the following relation for the singular part of the free energy per spin, $f = \beta F/N$, in d dimensions

$$f'(K', H', H'_{\text{eff}}) = \ell^d f(K, H, H_{\text{eff}}). \tag{2.1}$$

The length rescaling factor ℓ is discussed further on. The magnetization is given by $m = -\partial f/\partial H$, so differentiating (2.1) with respect to H we find

$$m'(K', H', H'_{\text{eff}}) = \ell^{d-y_H} m(K, H, H_{\text{eff}}) \tag{2.2}$$

with $H' = \ell^{y_H} H$, where y_H is the scaling exponent of the field H. Expanding (2.2) to first order in H and H_{eff} gives

$$\chi'(K') = \ell^{d-2y_H} \chi(K) \tag{2.3}$$

$$\alpha' K' \tilde{\chi}'(K') = \alpha K \tilde{\chi}(K) \tag{2.4}$$

where

$$\chi(K) \equiv \left.\frac{\partial m(K,H,0)}{\partial H}\right|_{H=0} \tag{2.5}$$

$$\tilde{\chi}(K) \equiv \left.\frac{\partial m(K,0,H_{\text{eff}})}{\partial H_{\text{eff}}}\right|_{H_{\text{eff}}=0}. \tag{2.6}$$

In obtaining (2.4) m_0 is supposed to scale like m, i.e. $m_0' = \ell^{d-y_H} m_0$, which in turn gives $H_{\text{eff}}' = \alpha' K' m_0' = \alpha' K' m_0 \ell^{d-y_H}$.

If (2.4) has a fixed point $K' = K = K_c$, then (2.2) describes a scaling property of the magnetization near $K = K_c$ and $H = H_{\text{eff}} = 0$. This point is identified with the critical point, which is given by the equation

$$\alpha' \tilde{\chi}'(K_c) = \alpha \tilde{\chi}(K_c). \tag{2.7}$$

The scaling exponent y_H follows from (2.3) at $K' = K = K_c$. Because for the clusters that we use all spins are also boundary spins, we always have $\tilde{\chi}(K) = \chi(K)$. It then follows from (2.3) and (2.4) that y_H is given by

$$\ell^{2y_H} = \ell^d \frac{\chi(K_c)}{\chi'(K_c)} = \ell^d \frac{\alpha'}{\alpha}. \tag{2.8}$$

By differentiating (2.4) with respect to K at the fixed point one finds

$$\alpha' \left\{ \tilde{\chi}'(K_c) + K_c \left.\frac{\partial \tilde{\chi}'(K')}{\partial K'}\right|_{K'=K_c} \right\} \left.\frac{\partial K'}{\partial K}\right|_{K=K_c} = \alpha \left\{ \tilde{\chi}(K_c) + K_c \left.\frac{\partial \tilde{\chi}(K)}{\partial K}\right|_{K=K_c} \right\}. \tag{2.9}$$

The thermal exponent $y_T = 1/\nu$, defined by $\partial K'/\partial K|_{K=K_c} = \ell^{y_T}$, can be calculated from this equation.

It is not obvious what definition one should adopt for the length rescaling factor ℓ, especially for small clusters. We use the original choice of Indekeu *et al* which is based on the number of spins in the cluster, $\ell = (N/N')^{1/d}$. It is argued by Slotte [6] that the estimates of the critical exponents are improved if one considers the number of interactions instead, which leads to a different value for ℓ. We will comment on this in the discussion.

A refinement of the MFRG method was proposed by Indekeu *et al* [2], who showed that, for large clusters, the effective magnetization m_0 should scale like $m_0' = \ell^{y_{HS}} m_0$, with y_{HS} the scaling exponent for a surface field. Combining this relation with (2.2) leads to

$$\alpha' K' \tilde{\chi}'(K') = \ell^{d-y_H-y_{HS}} \alpha K \tilde{\chi}(K) \tag{2.10}$$

instead of (2.4), while (2.3) still holds. Because of the introduction of an extra unknown in (2.10), one needs two equations to determine both $d - y_H - y_{HS}$ and the fixed point self-consistently. These are obtained by considering three clusters of sizes N, N', and N'', and imposing the scaling relations

$$\begin{aligned} m'(K', H', H_{\text{eff}}') &= \ell_1^{d-y_H} m(K, H, H_{\text{eff}}) \\ m''(K'', H'', H_{\text{eff}}'') &= \ell_2^{d-y_H} m'(K', H', H_{\text{eff}}') \end{aligned} \tag{2.11}$$

and $m_0' = \ell_1^{y_{HS}} m_0$, $m_0'' = \ell_2^{y_{HS}} m_0'$. This leads to unique values for $d - y_H - y_{HS}$ and the fixed point, but for y_T, y_H, and y_{HS} one finds slightly different results from the two equations (2.11).

When applying this method to the *XXZ* model, several changes take place. First, different ordered phases can occur in this model. The magnetization m must then be replaced by the order parameter of the phase under consideration; this can be the magnetization in either the z-direction or in the xy-plane, or the staggered magnetization. The field H couples to the order parameter, so it can be a magnetic field along the z-axis or in the xy-plane, or a staggered field. In all cases, the order parameter is given by $m = -\partial f / \partial H$. Second, the single coupling constant K is replaced by the pair (K, K_z). One now finds a fixed line $K(K_z)$ in the space of the two coupling constants instead of a single fixed point. As in the case of phenomenological renormalization [7, 8], this fixed line converges to the critical line for large cluster sizes. The values of y_H and y_T one finds from (2.3) and (2.9) will in general depend on the ratio K_z/K. This dependence, which is not in accordance with universality, should disappear when the cluster sizes increase. In addition, the value one finds for y_T also depends on the way $\partial K'/\partial K$ is defined in the (K, K_z) plane. We will always take the derivative along a line K_z/K = constant, but for large enough clusters any choice should lead to the correct value [8].

3. Results of the two-cluster method

The clusters we use are shown in figure 1. With these clusters we apply the MFRG method to the two-dimensional triangular and square lattices, and to the three-dimensional cubic and FCC lattices. We start by employing the simpler scheme using two clusters, since that gives more possibilities to compare results for different sets of clusters. Also, it is reasonably well behaved, in contrast to the three-cluster scheme, which turns out to give unacceptable results in some cases when applied to the small clusters we use here.

On applying the two-cluster scheme to the Hamiltonian (1.1), one immediately notices a difference in the behaviour of $\tilde{\chi}(K)$ for the FI phase on the one hand, and the *XY* and AI phases on the other hand. In the FI phase, for the clusters in figure 1, $\tilde{\chi}(K)$ is monotonically increasing from one at $K = 0$ to some constant value for $K \to \infty$. In the AI and *XY* phases it has a maximum, after which it decreases to either zero (even N), or to some non-zero value (odd N). This reflects the fact that for the FI phase the ground state of a cluster has the largest 'susceptibility' $\tilde{\chi}$, while the ground states for the *XY* and AI phases have either $\tilde{\chi} = 0$, or a relatively small non-zero value. As a consequence, when comparing $\alpha\tilde{\chi}(K)$ for different clusters, as in (2.7), there can be additional fixed points apart from the one indicating the phase transition, caused by the re-crossing of $\alpha\tilde{\chi}(K)$ for large K. In most cases there is a clear distinction between a solution of (2.7) indicating the phase transition, which clearly moves towards some limit for larger clusters, and the other zeros, which do not have this scaling behaviour (see figure 2 where $\alpha\tilde{\chi}(K)$ is shown for the FCC lattice for various clusters). Moreover, these spurious zeros usually lie at such large values of K that they are far removed from the region where the phase transition takes place, and they will in general not show up in the phase diagrams shown. (An exception to this is the square lattice case, which is discussed further on.)

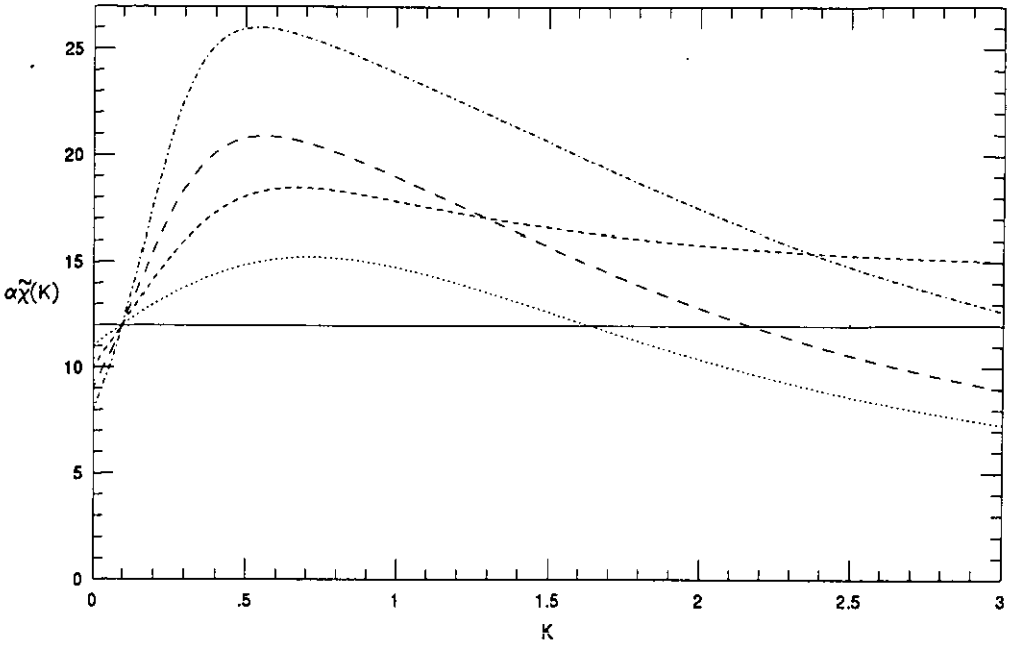

Figure 2. The behaviour of $\alpha\tilde{\chi}(K)$ for several clusters in the FCC lattice. $N = 1$ (——), $N = 2$ (·····), $N = 3$ (– – –), $N = 4$ (— — —), $N = 6$ (— · —). The intersections near $K = 0.1$ give the various approximations for K_c; the intersections at higher K are the additional fixed points discussed in the text.

3.1. The triangular lattice

The phase diagram obtained with the two-cluster method for the triangular lattice is shown in figure 3. Around $K = K_z = 0$ the system is in the disordered phase (D). When K_z is increased, ferromagnetic Ising order sets in (FI), while for increasing K the system enters the x–y ordered phase (XY). The parts of the phase diagram where an antiferromagnetic interaction dominates have been left blank, since we do not consider phases where frustration effects play a role. As was already shown in [3], the results for the FI boundary improve as the cluster size is increased. Although the critical coupling for the isotropic Heisenberg model ($K = K_z$) remains finite, it increases rapidly with cluster size, tending towards the exact result $K_c = \infty$. The XY phase boundary is also seen to move towards the series result for larger clusters [9].

The critical exponent y_T is shown in figure 4. Again, the result improves with increasing cluster size, roughly approaching the exact result $y_T = 1$ for the FI transition, $y_T = 0$ for the isotropic Heisenberg case, and the series result $y_T = 0.7$ for the XY phase [9]. Except for the region near $K = K_z$ where the cross-over between different values of y_T takes place, the dependence on the anisotropy is slight. From (2.8) it is seen that in the two-cluster method y_H does not depend on the coupling constants K and K_z. The best estimate for the triangular lattice ($N' = 2, N = 3$) gives $y_H = 1.55$, compared with the exact result $y_H = 1.875$ for the FI boundary, and a similar value from series expansions for the XY transition.

3.2. The square lattice

For the square lattice we obtain the phase diagram shown in figure 5. It also includes

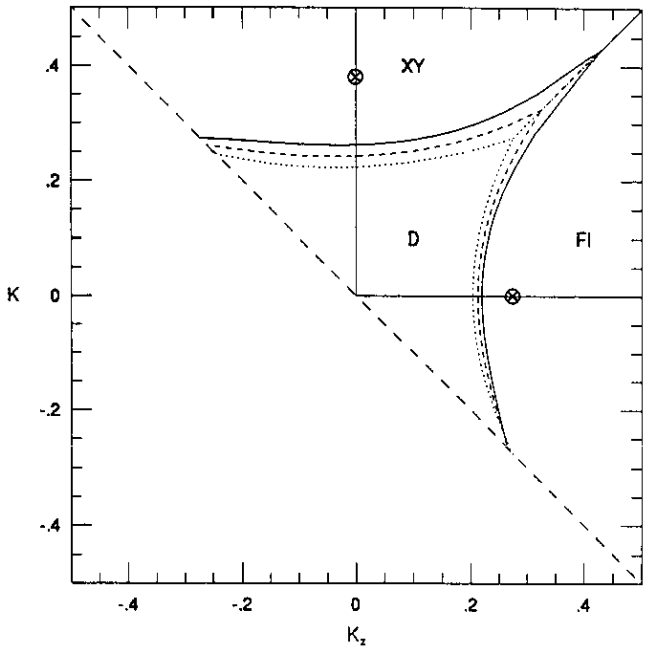

Figure 3. The phase diagram for the triangular lattice. The dotted curve is the result for $N' = 1, N = 2$, the broken curve for $N' = 1, N = 3$, and the full curve for $N' = 2, N = 3$. The crossed circles (⊗) represent exact and series expansion [9] results. The lower left half of the phase diagram, where the dominant interaction is antiferromagnetic and where frustration effects play a role, is not treated here.

the antiferromagnetic Ising phase (AI), which occurs for large negative K_z. We only plot the upper half of the phase diagram, which is symmetric under reflection in the line $K = 0$. Here again, the location of the FI boundary improves as the cluster sizes are increased. The isotropic Heisenberg model has $T_c = 0$, which is the exact result, for all cluster sizes. For the XY phase the spurious fixed points discussed above show up in the phase diagram. For the combinations $N' = 1, N = 2$ and $N' = 1, N = 4$ the XY phase boundary curves back for large K, thus suggesting that the system re-enters the disordered phase at low temperature. For these values of N' and N the MFRG for the XY phase does not have a fixed point at $T = 0$. Instead, for a constant ratio $K_z/K > -1$, there is, in addition to the repulsive fixed point indicating the phase transition, an attractive fixed point at lower T. As K_z/K is decreased towards -1 these points approach each other, and they eventually meet and are annihilated. The same happens for the AI phase where K_z/K approaches -1 from below. This leaves a gap in the phase diagram around $K_z \approx -K$. For $N' = 2, N = 4$ there *is* a fixed point at $T = 0$, so there is no re-entrance into the disordered phase. The gap around $K_z = -K$ has remained in roughly the same position, giving support to the conclusion that there is a region around $K_z = -K$, in this last approximation given by $-1.22 \lesssim K_z/K \lesssim -0.55$, where the disordered phase extends down to $T = 0$, flanked by XY and AI phases.

The results for the exponent y_T are similar to those for the triangular lattice, showing a reasonably flat plateau for the FI, AI, and XY phases, at values around respectively 0.8, 0.8, and 0.5 in the best approximation ($N' = 2, N = 4$), and in this case dropping to zero for the isotropic Heisenberg model and in the region

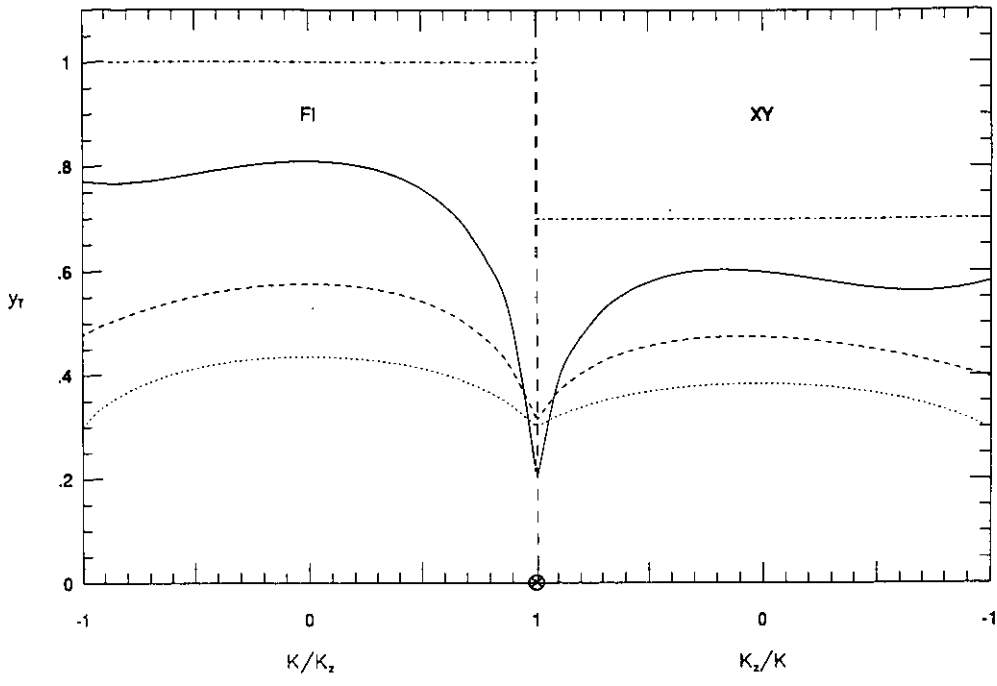

Figure 4. The exponent y_T for the triangular lattice, plotted along the phase boundaries in figure 3. The dotted curve is the result for $N' = 1, N = 2$, the broken curve for $N' = 1, N = 3$, and the full curve for $N' = 2, N = 3$. The exact and series [9] results are given by the chain curve and the crossed circle.

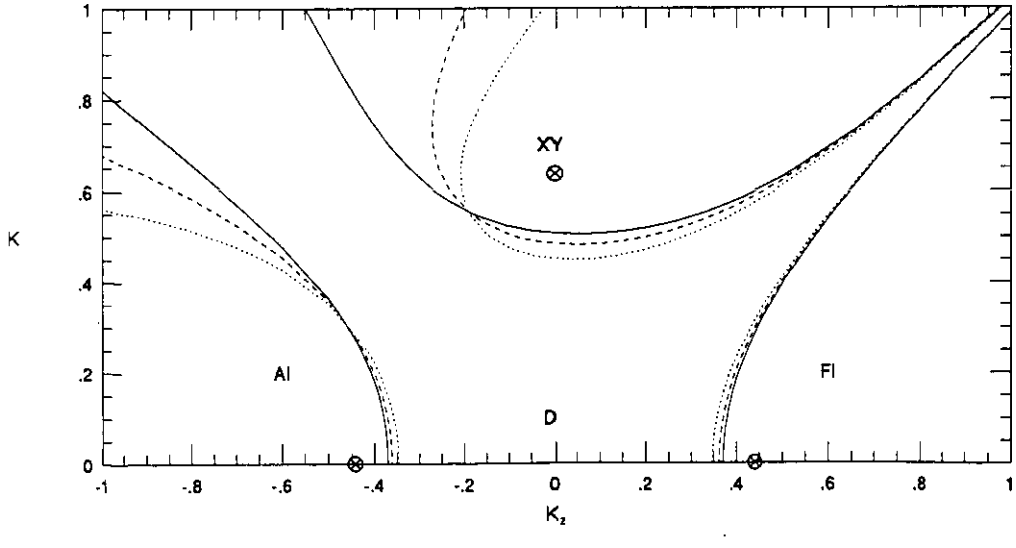

Figure 5. The phase diagram for the square lattice. The dotted curve is the result for $N' = 1, N = 2$, the broken curve for $N' = 1, N = 4$, and the full curve for $N' = 2, N = 4$. The crossed circles represent exact and series expansion results [9].

around $K = -K_z$. The best estimate for y_H gives $y_H = 1.59$.

3.3. The three-dimensional lattices

The phase diagrams for the three-dimensional lattices are shown in figures 6 and 7. For the cubic lattice there is some improvement as the cluster size is increased in most regions of the phase diagram. The exponent y_T again slowly varies along the phase boundary, assuming values of approximately 0.8, 0.7 and 0.6 for the FI, *XY* and isotropic Heisenberg transitions in the best estimate ($N' = 2, N = 4$), while for the magnetic exponent we find $y_H = 1.98$. As a comparison, field theoretical methods give $y_T = 1.59$, 1.49 and 1.42, respectively, and $y_H = 2.48$ [10].

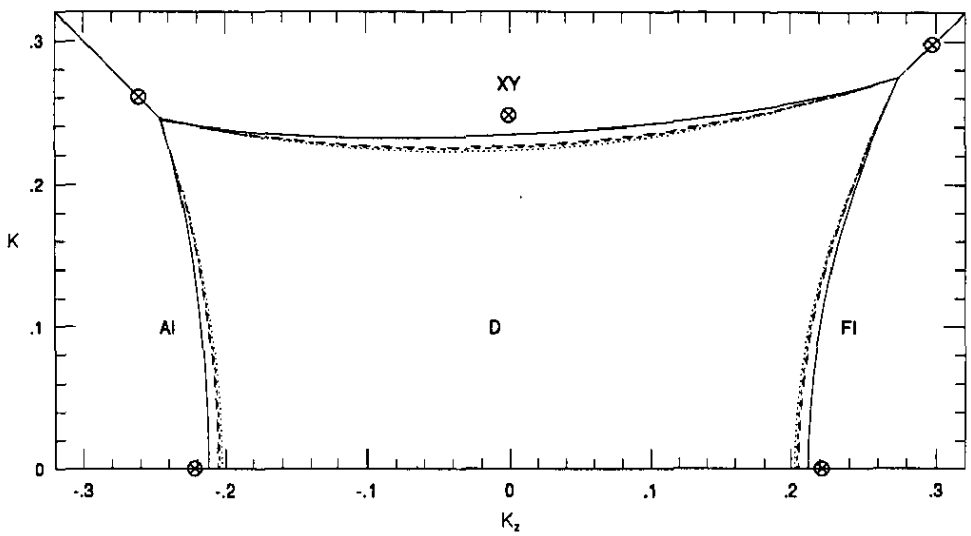

Figure 6. The phase diagram for the cubic lattice. The dotted curve is the result for $N' = 1, N = 2$, the short broken curve for $N' = 1, N = 4$, and the long broken curve for $N' = 2, N = 4$. Also included is the result of the three-cluster method discussed in section 4, with $N'' = 1, N' = 2, N = 4$ (full curve). The crossed circles represent the results of series expansions [11].

For the FCC lattice we find that, in contrast to the general trend, the inclusion of the largest cluster ($N = 6$) does not give better results. This confirms the observation that, especially in lattices with high coordination numbers, the improvement is not always monotonic as the cluster size is increased [2, 12]. For the exponents we find values that are slightly better than those for the cubic lattice.

4. Results of the three-cluster method

When applying the scheme using three clusters to the situations discussed above, one cannot *a priori* expect the results to be an improvement. Although this scheme does put the MFRG method on a sounder footing, and guarantees the convergence of large-cluster results, it is not necessarily an improvement for the small clusters used in the present calculation. In the first place, the assertion that the effective order parameter m_0 scales like a surface field only holds for large clusters. Second, whereas the location of K_c in the simpler method is independent of the length rescaling factor ℓ, in the three-cluster scheme it does depend on ℓ. The definition of ℓ for small clusters

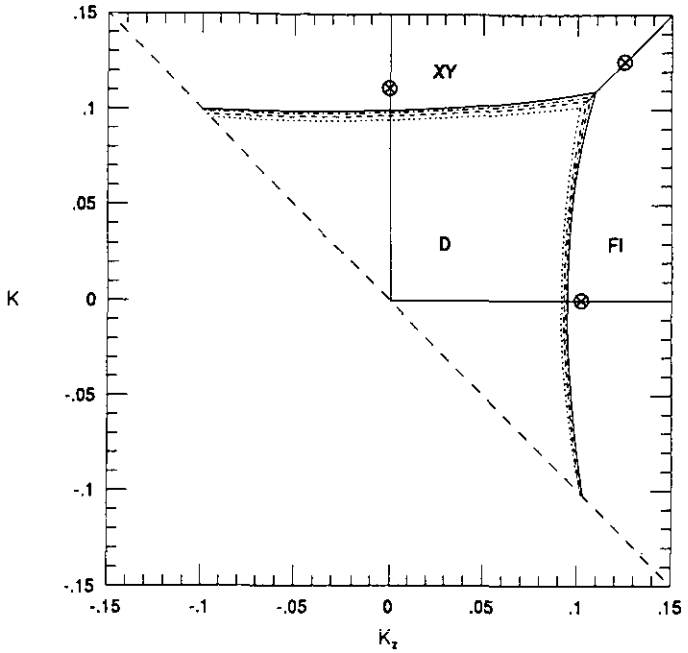

Figure 7. The phase diagram for the FCC lattice. The dotted curve is the result for $N' = 1, N = 2$, the broken curve for $N' = 2, N = 3$, the full curve for $N' = 3, N = 4$, and the chain curve for $N' = 4, N = 6$. The crossed circles represent the results of series expansions [11].

is rather arbitrary, and this arbitrariness affects the calculation of K_c. For very large clusters the exact definition of ℓ matters less, since there a variation of a few lattice spacings in the linear size of the cluster will not make a great deal of difference. For small clusters, however, a slight change in ℓ can give quite different results.

Especially for the XY and AI transitions the limitations of this scheme for small clusters will become apparent, since then also the large-K tails of $\tilde{\chi}(K)$ come into play. In those instances where the differences in the two-cluster scheme between the combinations N, N' and N', N'' are small, the three-cluster scheme will only give a slight shift in the location of the phase boundary. When the two combinations give results that are further apart, the three-cluster scheme will also give a large shift, and may not even lead to acceptable results.

A first instance of the difficulty of this more sophisticated scheme in dealing with small clusters is encountered for the triangular lattice. While the result for the FI boundary can be considered good, giving $K_c = 0.235$ for the pure Ising case, and shifting K_c for the isotropic Heisenberg model to infinity, even here we find some trouble, in the shape of an additional fixed point at high K, for the pure Ising model located at $K \approx 1.2$. This point can be dismissed as clearly being outside the region of the real phase transition; the same cannot be said of the phase boundary one finds for the XY phase. This line describes a zig-zag in the region between $K_z/K = 1$ and $K_z/K = -1$, which is clearly not a very sensible result. It shows that in this case the results of the three-cluster scheme for small clusters should not be taken too seriously. Similar behaviour is found for the square lattice, where the differences in behaviour for the various combinations of cluster sizes are even greater than for the

triangular lattice.

For the three-dimensional lattices the differences between the various combinations of clusters were rather small, and consequently the three-cluster method is better behaved for these lattices, only giving a small shift in the location of the phase boundary. For the cubic lattice, the resulting phase diagram is shown in figure 6, which does show an improvement over the two-cluster method. In contrast to the two-cluster case, (2.8) does not hold now, so the exponent y_H varies slightly along the phase boundary. Its value does not improve noticeably when compared with the previous results, and neither does the estimate for the exponent y_T. For the surface exponent one finds $y_{HS} \approx 1.1$, compared with the field theoretical value 0.8 [13].

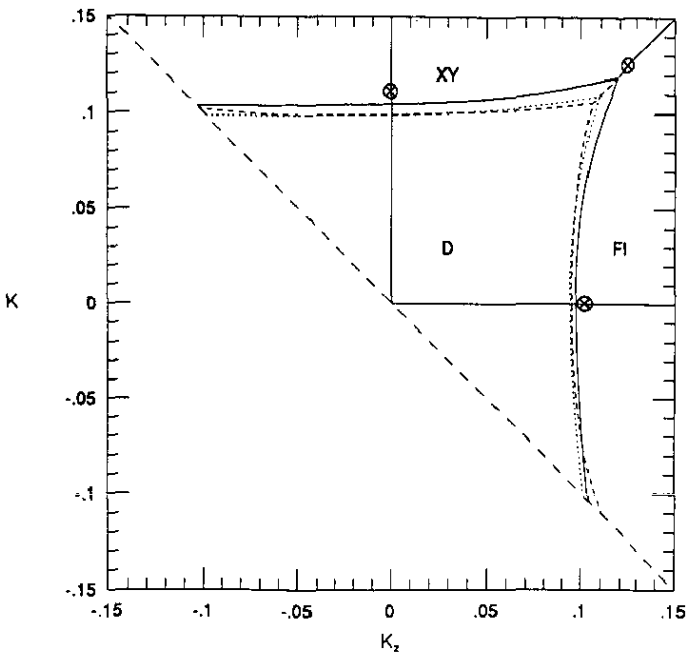

Figure 8. The phase diagram for the FCC lattice. The dotted curve is the result for $N'' = 1, N' = 2, N = 3$, the full curve for $N'' = 2, N' = 3, N = 4$, and the broken curve for $N'' = 2, N' = 4, N = 6$. The crossed circles represent the results of series expansions [11].

The phase diagram for the FCC lattice, figure 8, is also better than the result of the two-cluster method. As in the previous section, we see that the combination of the largest clusters does not necessarily give the best result. While for $N'' = 2, N' = 3, N = 4$ we find phase boundaries that are quite close to the series expansion estimates, the agreement becomes worse for $N'' = 2, N' = 4, N = 6$, and the combination $N'' = 3, N' = 4, N = 6$ fails to give a fixed line that one can identify with the phase boundary. The best estimates for the exponents are similar to those for the cubic lattice, and no great improvement over the two-cluster results.

5. Discussion

We have seen that applying the two-cluster version of the MFRG method to the

XXZ model leads to quite good results for the phase diagram. It is certainly an improvement over the mean-field approximation, which gives the critical lines $K = 1/z$ and $K_z = \pm 1/z$. Both the value of the critical coupling (see table 1 for an example) and the overall shape of the phase diagram are greatly improved when compared with this approximation. It is especially striking that for small clusters, where the computational effort is relatively small, the improvement over mean-field is already considerable. For larger clusters the results improve even further, but the convergence is not very fast. Also, especially for lattices with a high coordination number, where there are many possible ways to form larger clusters, the improvement is not always monotonic [2, 12]. The critical exponents that one finds as a by-product of this method are only rough estimates; much more accurate values can be found by field-theoretical methods. The nature of the ordered phases is determined by the boundary condition employed to break the symmetry. So, the *XY* phase is an ordered phase with a non-zero magnetization, while it is known that two-dimensional *XY* models exhibit a different type of long range order. Nevertheless, the MFRG result can be expected to give some indication of the location of the phase boundary.

Table 1. The critical coupling K_c of a pure *XY*-model ($K_z = 0$) on a cubic lattice, according to the mean field (MF), two-cluster MFRG (MFRG2 N', N), three-cluster MFRG (MFRG3) approximations, and the series result [11].

	MF	MFRG2 1,2	MFRG2 1,4	MFRG2 2,4	MFRG3 1,2,4	Series
K_c	0.167	0.224	0.226	0.227	0.235	0.248

Thus the performance of the MFRG method for the *XXZ* model, which exhibits different types of ordering, and is an essentially quantum mechanical model, is about the same as for the classical Ising model. There are some differences, though, which mostly become apparent at low temperatures. For the *XY* and AI phases one might find additional fixed points, as discussed in section 3. These points lie at high values of K, and usually do not interfere with the phase diagram. But for low dimensions and/or low coordination numbers, when K_c itself is relatively high, as in the case of the square lattice, they do show up in the phase diagram for some combinations of clusters. Even there, the phase boundaries one finds for these clusters are not radically different from what one finds for a combination that does not lead to additional fixed points. It may be remarked that the appearance of spurious zeros is also noticed in the pair approximation of the cluster variation method [14, 15]. In fact, the case $N' = 1, N = 2$ of the MFRG is equivalent to this approximation, just as for the classical pure Ising model it is equivalent to the Bethe–Peierls approximation.

The three-cluster version of the MFRG method is less successful for the *XXZ* model. One reason for this is that the method is geared to the use of large clusters; neither the introduction of a surface exponent y_{HS} nor the role played by the length rescaling factor ℓ are compatible with the use of small clusters. If one examines the values of y_H and y_{HS} for the three-dimensional lattices, one finds that $y_{HS} \approx d - y_H$, which is the relation that would follow from the method without a surface exponent. So for small clusters the effective field does not really scale as a surface field. Also, the arbitrariness in defining ℓ for small clusters affects the location of the phase boundary.

In the case of the *XXZ* model there is the extra complication of the spurious

fixed points that occur at high K. Especially for the two-dimensional lattices, where they are closest to the region of the phase transition, this has an effect on the calculation of the phase boundary. For example, combining the approximations with $N' = 1, N = 2$ and $N' = 2, N = 4$ for the square lattice, which behave differently for large K, cannot be expected to give a consistent result. In three dimensions the influence of these fixed points is less noticeable, since they are farther removed from K_c.

A suggestion has been made [6] for a different estimate for ℓ, which would improve the value for the exponents. According to this definition, one should consider the number of interactions in a cluster, including the ones with the surrounding effective magnetization. The resulting value for ℓ is in general smaller than the one following from the definition that we used, and consequently the exponents are larger and closer to the expected values. However, if one tries to use this new definition of ℓ in the three-cluster scheme, where the location of the phase boundary depends on it, the phase diagram is totally distorted and the original definition turns out to be far superior.

Acknowledgments

One of the authors (DJB) thanks Dr J O Indekeu for useful and stimulating discussions, and the Katholieke Universiteit Leuven for its hospitality. Part of this research was supported by the 'Stichting voor Fundamenteel Onderzoek der Materie' (FOM) which is financially supported by the 'Stichting Nederlands Wetenschappelijk Onderzoek' (NWO).

References

[1] Indekeu J O, Maritan A and Stella A L 1982 *J. Phys. A: Math. Gen.* **15** L291
[2] Indekeu J O, Maritan A and Stella A L 1987 *Phys. Rev.* B **35** 305
[3] Plascak J A 1984 *J. Phys. A: Math. Gen.* **17** L597
[4] Matsubara T and Matsuda H 1956 *Prog. Theor. Phys.* **16** 569
Matsuda H and Matsubara T 1957 *Prog. Theor. Phys.* **17** 19
[5] Fisher M E 1967 *Rep. Prog. Phys.* **30** 615
[6] Slotte P A 1987 *J. Phys. A: Math. Gen.* **20** L177
[7] Nightingale M P 1976 *Physica* **83A** 561
[8] Burkhardt T W and van Leeuwen J M J 1982 *Real Space Renormalization* ed T W Burkhardt and J M J van Leeuwen (Berlin: Springer)
[9] Rogiers J, Grundke E W and Betts D D 1979 *Can. J. Phys.* **57** 1719
[10] Le Guillou J C and Zinn-Justin J 1980 *Phys. Rev.* B **21** 3976
[11] Domb C 1974 *Phase Transitions and Critical Phenomena* vol 3, ed C Domb and M S Green (London: Academic)
Betts D D 1974 *Phase Transitions and Critical Phenomena* vol 3, ed C Domb and M S Green (London: Academic)
Rushbrooke G S, Baker G A Jr, and Wood P J 1974 *Phase Transitions and Critical Phenomena* vol 3, ed C Domb and M S Green (London: Academic)
[12] Indekeu J O private communication
[13] Diehl H W 1986 *Phase Transitions and Critical Phenomena* vol 10, ed C Domb and J L Lebowitz (London: Academic)
[14] Katsura S and Shimada K 1980 *Phys. Status Solidi* b **102** 163
[15] Bukman D J, An G and van Leeuwen J M L 1991 *Phys. Rev.* B **43** 13352